HHS Public Access

Author manuscript

J Immunol. Author manuscript; available in PMC 2016 November 01.

Published in final edited form as:

J Immunol. 2015 November 1; 195(9): 4492–4502. doi:10.4049/jimmunol.1500665.

Differential roles of Phospholipase D proteins in FcεRI-mediated signaling and mast cell function

Minghua Zhu, **Jianwei Zou**, **Tieshi Li**, **Sarah A. O'Brien**, **Yao Zhang**, **Sarah Ogden**, and **Weiguo Zhang***

Department of Immunology, Duke University Medical Center, Durham, NC 27710, USA

Abstract

Phospholipase D proteins (PLD)s are enzymes that catalyze the hydrolysis of phosphatidylcholine (PC) to generate an important signaling lipid, phosphatidic acid (PA). PA is a putative second messenger implicated in the regulation of vesicular trafficking and cytoskeletal reorganization. Previous studies using inhibitors and overexpression of PLD proteins have indicated that PLD1 and PLD2 play positive roles in FcεRI-mediated signaling and mast cell function. Here we used mice deficient in PLD1, PLD2, or both to study the function of these enzymes in mast cells. In contrast to published studies, we found that PLD1 deficiency impaired FcεRI-mediated mast cell degranulation; however, PLD2 deficiency enhanced it. Further biochemical analysis showed that PLD deficiency affected activation of the PI3K pathway and RhoA. Furthermore, our data indicated that while PLD1 deficiency impaired F-actin disassembly, PLD2 deficiency enhance microtubule formation. Together, our results suggested that PLD1 and PLD2, two proteins that catalyze the same enzymatic reaction, regulate different steps in mast cell degranulation.

Keywords

mast cells; degranulation; PI3K pathway; signal transduction

Introduction

Engagement of the high affinity IgE receptor (FcεRI) on the surface of mast cells initiates a series of biochemical events, leading to degranulation and anaphylactic reactions (1-3). The aggregation of the FcεRI first results in a rapid phosphorylation of the tyrosine residues within the immunoreceptor tyrosine-based activation motifs (ITAMs) of the FcεRI β and γ chains by Src family tyrosine kinases (PTK), Lyn and Fyn. Syk is then recruited to the receptor though binding the phosphorylated ITAMs via its tandem SH2 domains and is further activated. These activated tyrosine kinases then further phosphorylate LAT (Linker for Activation of T cells), LAB (Linker for Activation of B cells)/NTAL, and other signaling proteins, such as SLP-76 and PLC-γ1/PLC-γ2 (2, 4, 5). In mast cells, both LAT and LAB serve as scaffolds to recruit cytosolic adaptor molecules, such as Grb2, Gads, SLP-76, and

* Correspondence should be addressed to W.Z., Mailing address: Box 3010, Department of Immunology, Duke University Medical Center, Durham, NC 27710, US, zhang033@mc.duke.edu, Phone: (919)-613-7803, Fax: (919)-684-8982.

Disclosures

The authors have no financial conflicts of interest.

PLC-γ1/PLC-γ2 (4, 6). The formation of these signaling complexes at the membrane activates downstream signal cascades, such as Ras-MAPK activation and calcium flux, eventually leading to mast cell degranulation and cytokine production.

PLD (phospholipase D) proteins belong to one of the protein families containing a PH domain. These enzymes catalyze the hydrolysis of phosphatidylcholine (PC), the major membrane phospholipid, to produce phosphatidic acid (PA) and the water-soluble choline. PA is a putative second messenger that is likely involved in vesicular trafficking and cytoskeletal reorganization (7-9). It also binds several important signaling proteins, such as Raf and mTOR, to regulate their activation (10, 11). PLD proteins are expressed ubiquitously in different cell types or tissues. Studies in the past decade demonstrate that PLD proteins play important roles in FcεRI-mediated signaling and mast cell function. It has been shown that two members of the PLD family, PLD1 and PLD2, are required for FcεR-mediated mast activation and function (12-17). Even though these two proteins share similar sequences and structural domains, they have different subcellular localization. PLD1 is primarily localized to the secretory granules; however, it redistributes to the plasma membrane after stimulation. In contrast, PLD2 is present at the plasma membrane (14). It has been shown that following the engagement of the FcεRI, PLD1 and PLD2 are activated and potentially regulate multiple steps during exocytosis of granules. Although the importance of PLD proteins in FcεRI-mediated signaling and mast cell function has been implicated in previous studies, most of these studies rely heavily on the use of primary alcohols as inhibitors or overexpression of WT or mutant forms of PLDs in mast cell lines (12-15). Primary alcohols, which inhibit PA production by diverting production of phosphatidic acid to the corresponding phosphatidyl alcohol, are able to inhibit FcεRI-mediated degranulation. The caveat for these studies is that both primary alcohols and overexpression of PLD1 or PLD2 protein may have off-target effects. Thus, previous results on the role of PLD proteins in FcεRI-mediated signaling and mast cell function need to be confirmed.

In this study, we generated PLD1$^{-/-}$ and PLD2$^{-/-}$ mice to study the function of PLD proteins in FcεRI-mediated signaling and mast cell degranulation *in vivo* and *in vitro*. In contrast to published studies, which suggest that PLD1 and PLD2 proteins play positive roles in mast cells, we found that PLD1 and PLD2 function differently. While PLD1-defeciency impaired FcεRI-mediated signaling and mast cell function, PLD2 deficiency actually enhanced these pathways. Our data indicated that PLD proteins are indeed important in the regulation of mast cell function and allergic responses.

Materials and Methods

Mice

The FLP-FRT and Cre-loxP systems were used to generate PLD1 and PLD2-deficient mice (Fig.1). ES cells were targeted and injected into 129/Sv blastocysts to generate chimeric mice, which were crossed with FLP transgenic mice to delete the *neo* gene. After removal of the neo gene, exon 11 of *PLD1* and exons 11 and 12 of *PLD2* were floxed by two LoxP sites. To delete these exons, floxed mice were further crossed with the actin-Cre transgenic mice (the Jackson Laboratory) to generate PLD1$^{-/-}$ and PLD2$^{-/-}$ mice, which were

backcrossed with C57BL/6 mice for at least ten generations before analysis. dKO mice ($PLD1^{-/-}PLD2^{-/-}$) were generated by crossing $PLD1^{-/-}$ with $PLD2^{-/-}$ mice. All mice were used in accordance with the National Institutes of Health guidelines. The experiments described in this study were reviewed and approved by the Duke University Institutional Animal Care Committee. Mice were housed in specific pathogen-free conditions.

Antibodies and flow cytometry analysis

The following antibodies were used for Western blotting: anti-pTyr (4G10), Rac1 (Millipore), anti p-PLC-γ1, pAkt, Akt, pErk, pp38, p38, pJnk, pPDK1, PDK1, pp70S6K, p70S6K, cofilin, p-cofilin (Cell Signaling), and anti-Erk2, Jnk1, RhoA, Vav, PLD1, PLD2 (Santa Cruz Biotechnology). Antibodies used in FACS analysis were the following: APC-conjugated anti-c-Kit, PE-Cy7-anti-FcεRIα, PE-anti-CD107a, PE-anti-IL-6, FITC-anti-TNF-α (Biolegend). Flow cytometry was performed using the Becton Dickinson FACS Canto and analyzed by the FlowJo software.

BMMC culture, degranulation, activation, and Western blotting

Mast cells were derived from bone marrow cells harvested from $PLD1^{-/-}$, $PLD2^{-/-}$, dKO, and WT mice in IMDM supplemented with 10% fetal bovine serum and recombinant IL-3 (5ng/ml). After cultured in the IL-3 medium for 3 weeks, cells were analyzed by FACS analysis for FcεRIα and c-Kit expression to examine their purity. Degranulation of BMMCs was determined by measuring the release of β-hexosaminidase as previously described (4). Anti-DNP IgE (1 μg/ml, SPE-7 mAb, Sigma) or anti-TNP IgE (1μg/ml, C48-2, BD Biosciences) were used to sensitized cells in IMDM medium without IL-3 for 4-6 h. Cells then were stimulated with DNPHSA (1-1000 ng/ml) or TNP-BSA (10 -10,000 ng/ml) for the indicated time points.

For biochemical analysis, BMMCs ($2–5 \times 10^6$/ml) were sensitized with anti-DNP IgE (1 μg/ml, SPE-7 mAb, Sigma) in IMDM medium without IL-3 for 4-6 h, washed with IMDM, and then stimulated with DNP-HSA (30-100 ng/ml) for the indicated time points. A total of 1×10^7 cells were lysed in 500 μl of ice-cold RIPA lysis buffer (1% Triton, 0.5% sodium deoxycholic acid, 0.1% SDS, 25 mM Tris-Cl, pH 7.6, 150 mM NaCl, 5 mM EDTA, 1 mM Na_3VO_4). For Western blotting analysis, lysates were resolved on SDS-PAGE and transferred to nitrocellulose membranes. After incubation with primary antibodies, membranes were washed three times and probed with either anti-mouse, rabbit, or goat Ig conjugated to AlexaFluor 680 or IRDye800. Membranes were then visualized with the LI-COR Bioscience Odyssey system (LI-COR).

Calcium flux

BMMCs ($2–5 \times 10^6$/ml) were preloaded with anti-DNP IgE (1 μg/ml) in IMDM medium without IL-3 for 4 h. Cells were washed twice with Tyrode buffer and then loaded with Indo-1 (Molecular Probes) in the presence of 2mM EGTA for 30 min. Cells were washed again and further incubated in IMDM with EGTA for 30 min. DNP-HSA (30 ng/ml) was used to induce intracellular Ca^{2+} mobilization followed by adding 20mM CaCl2 for extracellular Ca^{2+} flux. Thapsigargin (1 μM) was also used to induce calcium flux in these cells. The fluorescence emission ratio at 405–495 nm was monitored by flow cytometry.

Passive Systemic Anaphylaxis

Mice were first sensitized with 2 μg of anti-DNP-IgE by intravenous injection for 20–24 h. They were then injected intravenously with 500 μg of DNP-HSA for 1.5 min. Mice were euthanized with CO_2 and blood was immediately collected by cardiac puncture. The histamine concentration in serum was determined using a competitive histamine enzyme-linked immunosorbent assay kit (Immunotech).

PLD activity assay

BMMCs were sensitized in 1 μg/ml anti-DNP IgE for 4–6 h followed by stimulation with 100 ng/ml of DNP-HSA for 5min. The cells were lyzed in 1% Triton lysis buffer (1% Triton, 25 mM Tris-Cl, pH 7.6, 150 mM NaCl, 5 mM EDTA, and protease inhibitors, 20μl lysis buffer for 2×10^6 cells). An Amplex Red PLD assay kit (Molecular Probes) was used to measure PLD activity. The lysates were diluted in 1X reaction buffer in the kit. The diluted lysates were mixed with the same volume of Amplex Red working solution. The PLD activity was determined by measuring fluorescence intensity after 30-60 min incubation at 37°C in the dark. The relative PLD activity was determined by subtracting the background fluorescence of the control without cell lysates.

Detection of Cytokine Production

BMMCs were sensitized in 1 μg/ml anti-DNP IgE for 4–6 h followed by stimulation with 100 ng/ml of DNP-HSA for 1 h. Total RNAs were isolated with the Trizol reagent (Invitrogen). cDNAs were synthesized with the SuperScript reverse transcriptase (Invitrogen) using oligo-dT as the primer. Quantification of cytokine RNAs was performed by real-time PCR with SYBR Green Super mix (Bio-Rad). The primers used to amplify cytokine cDNAs were described previously (4). Cytokines produced in the supernatant were quantitated by ELISA (Biolegend). Expression of IL-6 and TNF-α was also analyzed by intracellular staining, followed by FACS analysis.

Rac1 and RhoA activation

2×10^7/ml BMMCs were lysed in the lysis buffer (1% Triton, 25 mM Hepes, pH 7.5, 10% glycerol, 150 mM NaCl, 10 mM MgCl2, 1 mM EDTA, and protease inhibitors). The constructs expressing GST-Rhotekin RBD and GST-PAK-PBD fusion proteins were provided by Dr. K. Burridge (University of North Carolina, Chapel Hill, NC). Rac1 and RhoA activation was examined by pull-down assays as described previously (18). Briefly, protein lysates were incubated with GST-PAK-PBD or GST-Rhotekin RBD for 1 hour to pull down GTP-bounded Rac1 and RhoA. The GST precipitates were resolved on SDS-PAGE and GTP-bounded Rac1 and RhoA were detected by Western blotting with anti-Rac1 and anti-RhoA antibodies.

Cytoskeletal rearrangement

BMMCs were sensitized with anti-DNP IgE and stimulated with 100ng/ml of DNP-HSA for 2 and 5 mins. Cells were immediately fixed with 4% paraformaldehyde for 30 min, followed by permeablilization in FACS buffer containing 0.1% saponin for 15 min at room temperature. Cells were then stained with anti-α-tubulin (Sigma-Aldrich) at 1:1000 dilution

at 4°C for 30 min, followed by staining with Alexa Fluor 488 goat anti-mouse IgG at 1:500 dilution, rhodamine phalloidin (Life Technology) at 1:500 dilution, and DAPI at 1:2000 dilution at 4°C for 20 min. After washing, stained cells were dropped onto polylysine-coated slides. Cells were mounted by using Fluoromount-G. Images were performed using Leica SP5 inverted confocal microscope.

Results

Generation of PLD1, PLD2 knockout mice

To study the function of PLD1 and PLD2 on mast cell development and function, we generated PLD1 and PLD2 conditional knockout mice by using the Cre-loxP systems because of their broad expression in different cell types or tissues. The FLP-FRT recombinase system was used to remove the neo gene in chimeric mice after successful targeting. Exon 11 of PLD1 and exons 11 and 12 of PLD2 were floxed by two Loxp sites (Fig.1A). After chimeric mice were crossed with mice in which Cre recombinase expression is driven by the β-actin promoter, these exons were deleted, leading to the generation of nonfunctional and truncated proteins. To reduce variations in their genetic background, $PLD1^{-/-}$ and $PLD2^{-/-}$ mice were backcrossed with C57BL/6 mice for more than 10 generations. PLD double knockout mice (dKO) were then generated by crossing $PLD1^{-/-}$ with $PLD2^{-/-}$mice. Despite the ubiquitous expression of PLD proteins, $PLD1^{-/-}$, $PLD2^{-/-}$, and dKO mice were surprisingly viable and had no apparent abnormality. The success of gene targeting was confirmed by PCR (data not shown) and by Western blotting of lysates from mast cells (BMMCs) derived from the bone marrow of these mice (Fig.1B). PLD1 protein was clearly absent in dKO and $PLD1^{-/-}$ BMMCs, while PLD2 was not detected in dKO and $PLD2^{-/-}$ BMMCs.

PLD1 and PLD2 in mast cell degranulation *in vivo*

To examine whether FcεRI-mediated mast cell function and allergic responses are affected by PLD1 and PLD2 deficiency *in vivo*, we performed a systemic anaphylaxis assay. $PLD1^{-/-}$, $PLD2^{-/-}$, dKO, and WT mice were first injected intravenously with monoclonal anti-DNP IgE. At 20–24 h after injection, these mice were further challenged with DNP-HSA to cross-link the FcεRI and to induce anaphylaxis. At 1.5 min after challenge, blood was collected for determination of histamine concentration by ELISA. As shown in Fig.2A, histamine concentration in the blood from $PLD2^{-/-}$ mice was significantly higher than that in WT mice ($p<0.01$); however, it was lower in $PLD1^{-/-}$ mice ($p<0.05$). Interestingly, dKO mice, which are deficient in both PLD1 and PLD, released histamine similarly to WT mice ($p=0.99$). We also determined the levels of IL-6, TNF-α, and MCP-1 (mast cell protease), three preformed mediators released by mast cells, at 30 and 180 mins after DNP-HSA challenge. As shown in Fig.2B, the concentrations of these mediators were reduced in $PLD1^{-/-}$ mice and were slightly reduced in dKO mice. In contrast, $PLD2^{-/-}$ mice released similar levels of these proteins to WT mice. These results indicated that PLD1 and PLD2 deficiency had differential effects on the release of granules and preformed mediators. The differences in granule release were not due to the impact of PLD deficiency on mast cell development. There were similar numbers of mast cells in the peritoneal cavities, ear skin,

and back skin of these mice (data not shown). These mast cells expressed comparable levels of FcεRIα and c-Kit, two surface markers for mast cells (Fig.2C).

PLD1 and PLD2 in BMMC function

To analyze the function of PLD1 and PLD2 in mast cells biochemically, we derived mast cells from the bone marrow cells of PLD1$^{-/-}$, PLD2$^{-/-}$, dKO, and WT mice. After culture in IL-3 medium for 3-4 weeks, more than 95% of cultured cells were c-Kit^{+}FcεRIα^{+}. These cells expressed similar levels of c-Kit and FcεRIα (Fig.3A), further indicating that PLD1 and PLD2 are dispensable for mast cell development both *in vivo* (Fig.2C) and *in vitro* (Fig. 3A).

We next determined the effect of PLD deficiency on FcεRI-mediated activation of PLD activity. A PLD assay kit (Amplex Red) was used to assay the production of choline indirectly after hydrolysis of phosphatidylcholine by PLD enzymes. As shown in Fig.3B, FcεRI engagement led to increased PLD activity in WT cells; however, there was no increase of PLD activity after stimulation of PLD1$^{-/-}$ cells. Defective PLD activation was also seen in dKO cells as expected. Surprisingly, PLD2$^{-/-}$ mast cells had a similar PLD activity as WT cells. This result suggested that increased PLD activity after engagement of the FcεRI on mast cells is likely contributed mostly by PLD1 activation.

PLD1 and PLD2 in BMMC degranulation

We next tested whether PLD1$^{-/-}$, PLD2$^{-/-}$, and dKO BMMCs could degranulate normally after activation through the FcεRI. BMMCs were first sensitized with anti-DNP IgE and then stimulated with different concentrations of DNP-HSA to induce degranulation, which was assayed by measuring the release of β-hexosaminidase by mast cells into the supernatant. As shown in Fig. 3C, FcεRI-evoked degranulation by PLD2$^{-/-}$ BMMCs was increased compared to WT ones; PLD1$^{-/-}$ BMMCs had decreased degranulation while dKO cells had similar degranulation to WT cells. As a control, degranulation induced by thapsigargin, which bypasses FcεRI-mediated proximal signaling events, was similar among different BMMCs (Fig. 3C, lower panel). This result was in agreement with the histamine release data *in vivo* (Fig.2A)

Exocytosis of mast cell granules leads to up-regulation of CD107a at the cell surface. We further confirmed the degranulation data by FACS analysis of CD107a expression at different time points after crosslinking with DNP-HSA. As shown in Fig.3D, PLD2$^{-/-}$ BMMCs had the highest percentage cells expressing CD107a while PLD1$^{-/-}$ BMMCs had the lowest. dKO and WT cells had similar CD107a expression. Since the anti-DNP IgE antibody (SPE-7) we used to sensitize mast cells in above experiments is thought to be highly cytokinergic and may have polyreactivity to autoantigens (19), we also used a poorly cytokinergic anti-TNP IgE (C48-2) for sensitization and TNP-BSA for crosslinking. As shown in Fig.3E and 3F, TNP-BSA induced degranulation of these mast cells was similar to that induced by DNP-HSA (Fig.3C and 3D). Together, these data indicated that while PLD1 played a positive role to regulate FcεRI-mediated mast cell degranulation, PLD2 played a negative role.

PLD in mast cell cytokine production

The release of different cytokines is an important outcome of mast cell activation. We next analyzed the effect of PLD deficiency on cytokine production. BMMCs were sensitized with anti-DNP IgE and further activated by cross-linking with DNP-HSA for 1 h. Total RNAs were then prepared from unstimulated or stimulated PLD1$^{-/-}$, PLD2$^{-/-}$, dKO, and WT cells. The levels of cytokine RNAs were quantitated by real-time PCR. As shown in Fig.4A, FcεRI engagement increased the transcription of IL-6 and TNF-α in WT cells. Compared with WT cells, PLD1$^{-/-}$ cells had a significant reduction in the production of these RNAs while PLD2$^{-/-}$ cells had increased production. Interesting, dKO cells produced the amounts of these cytokines similarly to WT cells. The changes in IL-6 and TNF-α production by these BMMCs were also confirmed by intracellular staining of IL-6 and TNF-α (Fig.4B). Additionally, we determined the concentration of these cytokines secreted into the supernatant by ELISA. PLD1$^{-/-}$ cells secreted less IL-6 and TNF-α while PLD2$^{-/-}$ cells produced more than WT cells (Fig.4C). Together, our *in vivo* and *in vitro* data indicated that while both PLD1 and PLD2 are not required in mast cell development, they play opposite roles in FcεRI-mediated mast cell systemic anaphylaxis, degranulation, and cytokine production.

PLD in FcεRI-mediated proximal signaling

Next we investigated which FcεRI-initiated signaling events were affected by PLD deficiency. BMMCs were first sensitized with anti-DNP IgE and then activated with DNP-HSA for 0, 2, and 10 mins. Total lysates were analyzed by Western blotting with different antibodies. FcεRI engagement activates Lyn, Fyn, and Syk tyrosine kinases, which then phosphorylate many signaling proteins. Anti-phosphotyrosine blotting showed that overall tyrosine phosphorylation of proteins in PLD1$^{-/-}$, PLD2$^{-/-}$, dKO, and WT cells was similar (Fig. 5A). It was shown that PLD2 may be directly involved in Syk activation (17). We assayed Syk activation by Western blotting with anti-pSyk. Syk phosphorylation was also similar in these cells. Activation of three MAPK pathways, Erk, p38, and JNK, was not affected either. Re-blotting with antibodies against non-phosphorylated forms of Erk, Jnk, and p38 showed that similar amounts of lysates were loaded in each lane (Fig.5B).

FcεRI engagement also induces phosphorylation of PLC-γ1 and PLC-γ2 and calcium flux. Western blotting with antibodies against phosphorylated PLC-γ1 and PLC-γ2 showed that they were phosphorylated similarly in PLD1$^{-/-}$, PLD2$^{-/-}$, dKO, and WT cells (Fig.5C). Next, we examined FcεRI-mediated intracellular calcium flux by FACS analysis. BMMCs were sensitized with anti-DNP IgE first, loaded with indo-1 in the presence of EGTA, and then stimulated by DNP-HSA or thapsigargin. For extracellular calcium flux, 20mM CaCl2 was added after initial stimulation. No difference on calcium flux in these cells was detected (Fig.5D).

The effect of PLD deficiency on the PI3K pathway

FcεRI engagement also leads to the recruitment of the p85 subunit of PI3K through Gab2, activation of PI3K, and production of PIP_3. After PI3K activation, PDK1 is relocated to the membrane by binding to PIP_3 and activated through intermolecular auto-phosphorylation. PDK1 then phosphorylates and activates AKT (20-22). We next analyzed the effect of PLD

deficiency on the PI3K pathway by Western blotting with antibodies against phosphorylated PDK1 and AKT. We consistently detected enhanced phosphorylation of PDK1 and AKT in PLD2$^{-/-}$ BMMCs after FcεRI-mediated stimulation and reduced phosphorylation of these proteins in PLD1$^{-/-}$ cells. p70S6K is one of the proteins downstream of AKT activation. Its phosphorylation was also increased in PLD2$^{-/-}$ cells; however, slightly reduced in PLD1$^{-/-}$ cells. Interestingly, phosphorylation of PDK1, AKT, and p70S6K in dKO and WT cells was similar (Fig.6). Together, our results indicated that deficiency in PLD1, PLD2, or both had no effect on FcεRI-mediated protein tyrosine phosphorylation, MAPK activation, and calcium mobilization; however, PLD1 and PLD2 played antagonistic roles in the regulation of PI3K activation.

PLD in FcεRI-mediated microtubule formation and F-actin disassembly

Microtubule formation and F-actin disassembly are important steps during mast cell degranulation after stimulation through the FcεRI (23). As we showed in Fig. 2A, 3C, and 3E, PLD1$^{-/-}$ mast cells had reduced degranulation while PLD2$^{-/-}$ cells had enhanced degranulation both *in vivo and in vitro*. Next, we examined the formation of microtubule network and disassembly of F-actin by staining BMMCs with anti-α-tubulin (green) and rhodaminephalloidin (red), respectively. As shown in Fig. 7A and 7B, after FcεRI stimulation, the green fluorescence for microtubule staining in WT cells was highest at 2 mins after stimulation. Before stimulation, a clear F-actin ring (the red fluorescence) was clearly seen in WT mast cells, but after stimulation, the red fluorescence was reduced due to the collapse of the F-actin ring. In PLD1$^{-/-}$ mast cells, microtubule formation was relatively normal compared with WT cells; however, F-actin disassembly was transient as the F-actin ring quickly re-formed by 5 mins after stimulation. In PLD2$^{-/-}$ mast cells, while F-actin disassembly was normal, microtubule formation was enhanced. Interestingly, in dKO cells, we observed an enhanced intensity of tubulin staining and transient F-actin disassembly. Thus, dKO cells had a combined phenotype of both PLD1$^{-/-}$ and PLD2$^{-/-}$ cells. This result suggested that PLD1 and PLD2 play different roles in mast cell degranulation. While PLD1 positively regulates the disassembly of F-actin ring, PLD2 negatively modulates microtubule formation.

An important molecule regulating the assembly and disassembly of F-actin is cofilin, an actin-depolymerizing factor (24). Upon engagement of the FcεRI, cofilin is dephosphorylated and promotes actin depolymerization. Ser-3 is the main phosphorylation site on cofilin. We determined the level of cofilin phosphorylation by immunoprecipitating cofilin followed by Western blotting with anti-phospho-cofilin. As shown in Fig.8A, phosphorylation of cofilin in WT cells decreased after 2 min of stimulation and stayed low at 5 mins. Cofilin was also dephosphorylated in PLD2$^{-/-}$ cells similarly to that in WT cells. Interestingly, after engagement of the FcεRI, cofilin was not dephosphorylated in PLD1$^{-/-}$ and dKO BMMCs, which had transient F-actin collapse (Fig.7). Western blotting using anti-cofilin showed that a similar amount of cofilin protein was immunoprecipitated from these cells. These data suggested that PLD1 functions in FcεRI-mediated mast cell degranulation through regulating cofilin dephosphorylation.

Rac and Rho GTPases play an important role in modulating the microtubule formation and degranulation in mast cells (23, 25). Vav is one of the guanine exchange factors (GEF) that catalyze activation of these small G proteins. Western blotting showed that phosphorylation of Vav was not altered in these PLD-deficient BMMCs (Fig.8B). We next examined the activation of Rac1 and RhoA by using GST-PAK-RBD and GST-Rhotekin-RBD to pull-down GTP-bound Rac1 and RhoA respectively. While Rac1 activation was similar in these cells (data not shown), RhoA activation was clearly enhanced in PLD2$^{-/-}$ cells and slightly reduced in PLD1$^{-/-}$ cells (Fig.8C). These data suggested that PLD2 negatively modulates RhoA activation and microtubule formation in mast cells.

Discussion

The function of PLDs in mast cells has been thoroughly explored previously. Published data have shown that primary alcohols could suppress FcεRI-mediated mast cell degranulation (12-14). The expression of the dominant negative (DN) form of PLD1 blocks granule translocation to the plasma membrane, whereas the expression of the DN form of PLD2 also blocks degranulation, suggesting that PLD1 and PLD2 have positive roles to regulate degranulation in mast cells (14). It has been also suggested that PLD activation leads to increased production of DAG, and therefore indirectly contributes to sustained PKC activation, which is important for degranulation. In RBL cells transfected with PLD1 and PLD2 siRNAs, DAG production, translocation of PKC, and degranulation are suppressed (15). These data suggest that PLDs facilitate the activation of PKC and degranulation in mast cells.

While above studies indicate that PLD1 and PLD2 proteins play positive roles in FcεRI-mediated signaling, other studies suggest that they may have different roles in mast cells. For example, in one study, expression of PLD2, either WT or DN form, has no effect on degranulation, whereas expression of the DN PLD1 protein enhances FcεRI-induced degranulation through increasing tyrosine phosphorylation of FcεRI subunits, Syk, and PLC-γ, and calcium mobilization (16). These data suggest that PLD1 negatively regulates FcεRI-mediated signaling and that PLD2 plays a minimal role. However, another study suggests a different role for PLD2. Overexpression of either WT or DN PLD2 enhances FcεRI-induced activation of Syk and phosphorylation of LAT and SLP-76. Knockdown of PLD2 in RBL cells blocks phosphorylation of these proteins. In addition, it was found that PLD2 could interact with Syk via its PX domain. Therefore, the authors proposed that PLD2 functions as an adaptor protein in the activation of Syk in mast cells (17). While these studies suggest that PLD proteins play important roles in the regulation of mast cell function, many of these experiments were done using the RBL cell line and inhibitors. The results from different groups vary and some even contradict each other. This is likely due to variations in the concentrations of inhibitors used, duration of treatment, or differences in the expression levels of WT and the DN forms of PLD1 and PLD2 proteins.

In this study, we used mice deficient in PLD1, PLD2, or both to study the function of these proteins in mast cells *in vivo* and *in vitro*. Our data clearly demonstrated that while these two proteins catalyze the same enzymatic reaction, their deficiencies had different effects on FcεRI-mediated signaling and mast cell function. Our data showed that PLD1 played a

positive role in mast cells as FcεRI-mediated histamine release and cytokine production by PLD1$^{-/-}$ mast cells were significantly reduced. In contrast, PLD2 acted as a negative regulator in these cells. FcεRI-mediated effector function in PLD2$^{-/-}$ mast cells was actually enhanced. Interestingly, mast cells deficient in both PLD1 and PLD2 were similar to WT cells.

To analyze how PLD deficiency affected mast cell degranulation and cytokine production, we performed a series of biochemical analysis of FcεRI-mediated signaling using BMMCs. Our data showed that FcεR-mediated proximal signaling events were not affected. Despite the fact that the published data suggest a role of PLD2 in FcεRI-mediated Syk activation and subsequent protein tyrosine phosphorylation (17), we did not observe significant differences in overall tyrosine phosphorylation of proteins, indicating that Syk activation is likely not affected in these cells. FcεRI-mediated activation of three MAPKs, Erk, Jnk, and p38, was also normal. In addition, we also detected normal PLC-γ1 and -γ2 phosphorylation and calcium mobilization. Together, these data suggested that neither PLD1 nor PLD2 is involved in FcεRI-mediated proximal signaling events. The reason why our data are different from the published data is not clear. This could be due to differences in cell lines, off-target effects of siRNA, overexpression, or potential compensatory mechanisms by PLD deficiency.

While FcεRI-mediated MAPK activation and calcium flux were normal, our data showed that PI3K activation was affected by PLD deficiency. Compared with WT cells, PLD2$^{-/-}$ cells had increased PDK1, AKT, and p70S6K phosphorylation while PLD1$^{-/-}$ cells had decreased phosphorylation of these proteins, suggesting that these two PLD proteins play opposite roles in the regulation of the PI3K pathway. PI3K activation leads to PI(3,4,5)P3 production, which recruits both Akt and PDK1 to the plasma membrane for activation. It has been shown that PLD1 and PLD2 have different subcellular localization. While PLD1 is mostly localized in the Golgi or perinuclear vesicles, PLD2 is mainly associated with the plasma membrane. Perhaps, PLD2 deficiency leads to increased PI(3,4,5)P3 production because there might be more PI(4,5)P2 locally available for PI3K. It is also possible that PLD2 functions as an adaptor independent of its enzymatic activity. This possibility is supported by our data showing that PLD2-deficiency had no effect on FcεRI-induced increase of PLD activity. On the other hand, PLD1 deficiency caused a reduction in PLD activity and impaired activation of the PI3K pathway. PLD1 has been suggested to contribute to mTORC1 activity through producing phosphatidic acid. PA has been reported to bind and activate mTORC1, although these data were largely done using overexpression or inhibitors (26). It is possible that PLD1 functions positively in FcεRI-mediated PI3K activation through production of PA.

Previous studies show that FcεRI engagement leads to Gab2 phosphorylation. Gab2 subsequently binds to the p85 subunit of PI3K and activates the PI3K pathway, which further activates RhoA and leads to microtubule formation(20, 23). The microtubule network is required for granule translocation to the plasma membrane. In PLD2$^{-/-}$ cells, FcεRI-mediated PI3K, RhoA activation, and microtubule formation were all enhanced. How PLD2 plays a negative role in these processes is not clear. Guanine exchange factors, such as Sos and Dok2, are well known to bind multiple lipids. Sos is recruited to the plasma

membrane via PI(4,5)P2 and PA, while Dok2, a GEF for Rac1, binds PI(3,4,5)P3 and PA. It has also been shown that GTPases, such as Rac1, can be recruited to the sites of stimulation via the interaction of their polybasic motifs with PA (27, 28). However, it is possible that this binding might not be highly specific as there are other acidic phospholipids, like PI(4,5)P2 and PI(3,4,5)P3 enriched in the plasma membrane. While it is possible that PA might be directly involved in the activation and recruitment of GTPases, we believe that PLD functions in this pathway through affecting PI3K activation.

Activation through the FcεRI induces cytoskeletal rearrangement that includes microtubule formation and disassembly of the F-actin ring. For granules to be released from mast cells, granules translocate and fuse with the plasma membrane before release. This process requires microtubule formation and collapse of F-actin ring. Interestingly, deficiency of PLD1 and PLD2 also had different effects on the microtubule formation and F-actin reorganization during degranulation. PLD1 deficiency caused a defect in F-actin disassembly as F-actin ring quickly reformed after FcεRI engagement; however, PLD2 enhanced microtubule formation as microtubule network was intensified in PLD2$^{-/-}$ cells (Fig.7). Cytoskeletal organization is regulated by Rac and Rho GTPases. Indeed, our data showed that RhoA activation was affected by PLD1 and PLD2 deficiency. Similar to PI3K activation, RhoA activation was enhanced in PLD2$^{-/-}$ cells, however, only slightly reduced in PLD1$^{-/-}$ cells. RhoA activation has been shown to be important for microtubule formation and degranulation in mast cells (23). Thus, PLD2 regulates microtubule formation and degranulation through RhoA.

Our data showed that PLD1 is important in F-actin disassembly as F-actin quickly reformed by FcεRI engagement in PLD1$^{-/-}$ and dKO cells. Cofilin plays an important role in controlling actin dynamics by catalyzing actin polymerization and depolymerization. Its activity is mainly regulated by phosphorylation at Ser3. It is mainly phosphorylated by LIM kinase and dephosphorylated by SSH1 or CIN phosphatase. The activity of SSH1 can be regulated by several proteins, such as calcineurin and CaMKII. PI3K can also promote SSH1 activation while PTEN decreases its activation in cancer cell lines (24). In WT mast cells, activation via the FcεRI induced dephosphorylation of cofilin (Fig.8), which promotes the collapse of F-actin ring. In PLD1$^{-/-}$ and dKO mast cells, dephosphorylation of cofilin appeared to be blocked, suggesting that PLD1 functions upstream of cofilin dephosphorylation. Because FcεRI-mediated calcium flux was normal in PLD1$^{-/-}$, PLD2$^{-/-}$, and dKO mast cells, calcineurin and CaMKII activation were most likely normal. Because we observed reduced PI3K activation in PLD1$^{-/-}$ cells, it is possible that in mast cells, PLD1 functions in SSH1 activation and further cofilin dephosphorylation through PI3K; however, this possibility was not supported by the data from dKO cells because cofilin dephosphorylation and F-actin disassembly were still affected despite that PI3K activation was normal. Thus, how PLD1 is involved in cofilin dephosphorylation remains to be explored in the future. Interestingly, it was shown previously that in muscarinic receptor signaling, upon phosphorylation by LIM-kinase, cofilin interacts with and activate PLD1, not PLD2 (29). Thus, PLD1 may also interact with phosphorylated cofilin in mast cells. This interaction may be required for recruiting phosphatases, such as SSH1, to dephosphorylate cofilin. It is also possible that the PLD1-cofilin interaction may change the conformation of cofilin to expose the phosphorylation sites for phosphatases.

One of surprising results from our study is that dKO mast cells were relatively normal compared with PLD1$^{-/-}$ and PLD2$^{-/-}$ cells. In dKO cells, there was no increased PLD activity after mast cell activation. PLD activation leads to production of choline and PA. PA is an important secondary messenger. In addition to PLD enzymes, PA can also be produced by DGK-catalyzed phosphorylation of diacylglycerol. DGK is a negative regulator of diacylglycerol-dependent signaling. DGKζ$^{-/-}$ mice are defective in mast cell function *in vivo*. DGKζ$^{-/-}$ BMMCs have impaired degranulation due to diminished phospholipase Cγ and calcium flux. In DGKζ$^{-/-}$ mast cells, FcεRI-mediated PA production is reduced, indicating that DGKζ also contributes to FcεRI-mediated PA production(30). Thus, it is possible that DGK can compensate for the loss of PLD1, PLD2, or both in these cells. This possibility will be studied in the future. In summary, our data clearly indicate that PLD1 and PLD2 are important in FcεRI-mediated signaling and regulate different steps during mast cell degranulation.

Acknowledgements

The authors thank the Duke University Cancer Center Flow Cytometry, DNA Sequencing, and Transgenic Mouse facilities for their excellent service.

This work was supported by National Institutes of Health Grant AI093717

Abbreviations used

PLD	Phospholipase D
PA	phosphatidic acid
DNP	dinitrophenol
TNP	trinitrophenol
HSA	human serum albumin
WT	wild-type
DN	dominant negative

References

1. Siraganian RP. Mast cell signal transduction from the high-affinity IgE receptor. Curr Opin Immunol. 2003; 15:639–646. [PubMed: 14630197]
2. Rivera J. Molecular adapters in Fc(epsilon)RI signaling and the allergic response. Curr Opin Immunol. 2002; 14:688–693. [PubMed: 12413516]
3. Kinet JP. The high-affinity IgE receptor (Fc epsilon RI): from physiology to pathology. Annu Rev Immunol. 1999; 17:931–972. [PubMed: 10358778]
4. Zhu M, Liu Y, Koonpaew S, Granillo O, Zhang W. Positive and negative regulation of FcepsilonRI-mediated signaling by the adaptor protein LAB/NTAL. J Exp Med. 2004; 200:991–1000. [PubMed: 15477350]
5. Brdicka T, Imrich M, Angelisova P, Brdickova N, Horvath O, Spicka J, Hilgert I, Luskova P, Draber P, Novak P, Engels N, Wienands J, Simeoni L, Osterreicher J, Aguado E, Malissen M, Schraven B, Horejsi V. Non-T cell activation linker (NTAL): a transmembrane adaptor protein involved in immunoreceptor signaling. J Exp Med. 2002; 196:1617–1626. [PubMed: 12486104]

6. Saitoh S, Arudchandran R, Manetz TS, Zhang W, Sommers CL, Love PE, Rivera J, Samelson LE. LAT is essential for Fc(epsilon)RI-mediated mast cell activation. Immunity. 2000; 12:525–535. [PubMed: 10843385]
7. Cockcroft S. Signalling roles of mammalian phospholipase D1 and D2. Cell Mol Life Sci. 2001; 58:1674–1687. [PubMed: 11706993]
8. Lehman N, Di Fulvio M, McCray N, Campos I, Tabatabaian F, Gomez-Cambronero J. Phagocyte cell migration is mediated by phospholipases PLD1 and PLD2. Blood. 2006; 108:3564–3572. [PubMed: 16873675]
9. Gomez-Cambronero J, Di Fulvio M, Knapek K. Umnderstanding phospholipase D (PLD) using leukocytes: PLD involvement in cell adhesion and chemotaxis. J Leukoc Biol. 2007; 82:272–281. [PubMed: 17431093]
10. Andresen BT, Rizzo MA, Shome K, Romero G. The role of phosphatidic acid in the regulation of the Ras/MEK/Erk signaling cascade. FEBS Lett. 2002; 531:65–68. [PubMed: 12401205]
11. Zhao C, Du G, Skowronek K, Frohman MA, Bar-Sagi D. Phospholipase D2-generated phosphatidic acid couples EGFR stimulation to Ras activation by Sos. Nat Cell Biol. 2007; 9:706–712. [PubMed: 17486115]
12. Chahdi A, Choi WS, Kim YM, Fraundorfer PF, Beaven MA. Serine/threonine protein kinases synergistically regulate phospholipase D1 and 2 and secretion in RBL-2H3 mast cells. Mol Immunol. 2002; 38:1269–1276. [PubMed: 12217394]
13. Brown FD, Thompson N, Saqib KM, Clark JM, Powner D, Thompson NT, Solari R, Wakelam MJ. Phospholipase D1 localises to secretory granules and lysosomes and is plasma-membrane translocated on cellular stimulation. Curr Biol. 1998; 8:835–838. [PubMed: 9663393]
14. Choi WS, Kim YM, Combs C, Frohman MA, Beaven MA. Phospholipases D1 and D2 regulate different phases of exocytosis in mast cells. J Immunol. 2002; 168:5682–5689. [PubMed: 12023367]
15. Peng Z, Beaven MA. An essential role for phospholipase D in the activation of protein kinase C and degranulation in mast cells. J Immunol. 2005; 174:5201–5208. [PubMed: 15843515]
16. Hitomi T, Zhang J, Nicoletti LM, Grodzki AC, Jamur MC, Oliver C, Siraganian RP. Phospholipase D1 regulates high-affinity IgE receptor-induced mast cell degranulation. Blood. 2004; 104:4122–4128. [PubMed: 15339843]
17. Lee JH, Kim YM, Kim NW, Kim JW, Her E, Kim BK, Kim JH, Ryu SH, Park JW, Seo DW, Han JW, Beaven MA, Choi WS. Phospholipase D2 acts as an essential adaptor protein in the activation of Syk in antigen-stimulated mast cells. Blood. 2006; 108:956964.
18. Liu BP, Burridge K. Vav2 activates Rac1, Cdc42, and RhoA downstream from growth factor receptors but not beta1 integrins. Mol Cell Biol. 2000; 20:7160–7169. [PubMed: 10982832]
19. Kashiwakura J, Okayama Y, Furue M, Kabashima K, Shimada S, Ra C, Siraganian RP, Kawakami Y, Kawakami T. Most Highly Cytokinergic IgEs Have Polyreactivity to Autoantigens. Allergy Asthma Immunol Res. 2012; 4:332–340. [PubMed: 23115729]
20. Gu H, Saito K, Klaman LD, Shen J, Fleming T, Wang Y, Pratt JC, Lin G, Lim B, Kinet J-P, Neel BG. Essential role for Gab2 in the allergic response. Nature. 2001; 412:186–190. [PubMed: 11449275]
21. Ali K, Bilancio A, Thomas M, Pearce W, Gilfillan AM, Tkaczyk C, Kuehn N, Gray A, Giddings J, Peskett E, Fox R, Bruce I, Walker C, Sawyer C, Okkenhaug K, Finan P, Vanhaesebroeck B. Essential role for the p110delta phosphoinositide 3-kinase in the allergic response. Nature. 2004; 431:1007–1011. [PubMed: 15496927]
22. Barker SA, Caldwell KK, Hall A, Martinez AM, Pfeiffer JR, Oliver JM, Wilson BS. Wortmannin blocks lipid and protein kinase activities associated with PI 3-kinase and inhibits a subset of responses induced by Fc epsilon R1 cross-linking. Mol Biol Cell. 1995; 6:1145–1158. [PubMed: 8534912]
23. Nishida K, Yamasaki S, Ito Y, Kabu K, Hattori K, Tezuka T, Nishizumi H, Kitamura D, Goitsuka R, Geha RS, Yamamoto T, Yagi T, Hirano T. Fc{epsilon}RI-mediated mast cell degranulation requires calcium-independent microtubule-dependent translocation of granules to the plasma membrane. J Cell Biol. 2005; 170:115–126. [PubMed: 15998803]

24. Bravo-Cordero JJ, Magalhaes MA, Eddy RJ, Hodgson L, Condeelis J. Functions of cofilin in cell locomotion and invasion. Nat Rev Mol Cell Biol. 2013; 14:405–415. [PubMed: 23778968]
25. Etienne-Manneville S, Hall A. Rho GTPases in cell biology. 2002; 420:629–635.
26. Fang Y, Vilella-Bach M, Bachmann R, Flanigan A, Chen J. Phosphatidic acid-mediated mitogenic activation of mTOR signaling. Science. 2001; 294:1942–1945. [PubMed: 11729323]
27. Zhang Y, Du G. Phosphatidic acid signaling regulation of Ras superfamily of small guanosine triphosphatases. Biochim Biophys Acta. 2009; 1791:850–855. [PubMed: 19540930]
28. Chae YC, Kim JH, Kim KL, Kim HW, Lee HY, Heo WD, Meyer T, Suh PG, Ryu SH. Phospholipase D activity regulates integrin-mediated cell spreading and migration by inducing GTP-Rac translocation to the plasma membrane. Mol Biol Cell. 2008; 19:3111–3123. [PubMed: 18480413]
29. Han L, Stope MB, de Jesus ML, Oude Weernink PA, Urban M, Wieland T, Rosskopf D, Mizuno K, Jakobs KH, Schmidt M. Direct stimulation of receptor-controlled phospholipase D1 by phospho-cofilin. EMBO J. 2007; 26:4189–4202. [PubMed: 17853892]
30. Olenchock BA, Guo R, Silverman MA, Wu JN, Carpenter JH, Koretzky GA, Zhong XP. Impaired degranulation but enhanced cytokine production after Fc epsilonRI stimulation of diacylglycerol kinase zeta-deficient mast cells. J Exp Med. 2006; 203:1471–1480. [PubMed: 16717114]

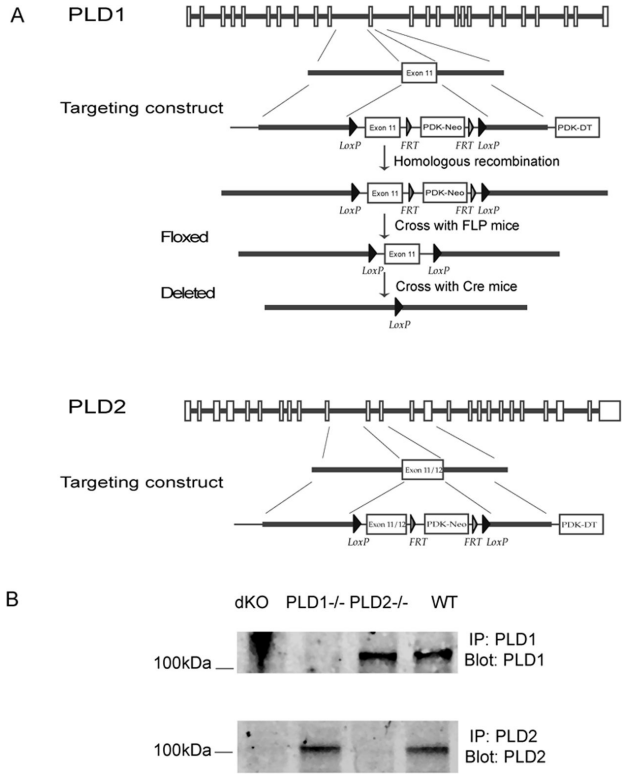

Figure 1.

Generation of PLD1$^{-/-}$ and PLD2$^{-/-}$ mice. (A). Targeting constructs. The *neo* gene was removed by the FLP recombinase. The Cre-loxP system was used to delete exon 11 of PLD1 or exons 11 and 12 of PLD2. These exons were floxed by two LoxP sites. (B). Absence of PLD1 and PLD2 protein in PLD-deficient mice. BMMCs derived from the bone marrow cells of dKO (PLD1$^{-/-}$PLD2$^{-/-}$), PLD1$^{-/-}$, PLD2$^{-/-}$, and WT mice were analyzed by Western blotting after anti-PLD1 and anti-PLD2 immunoprecipitation.

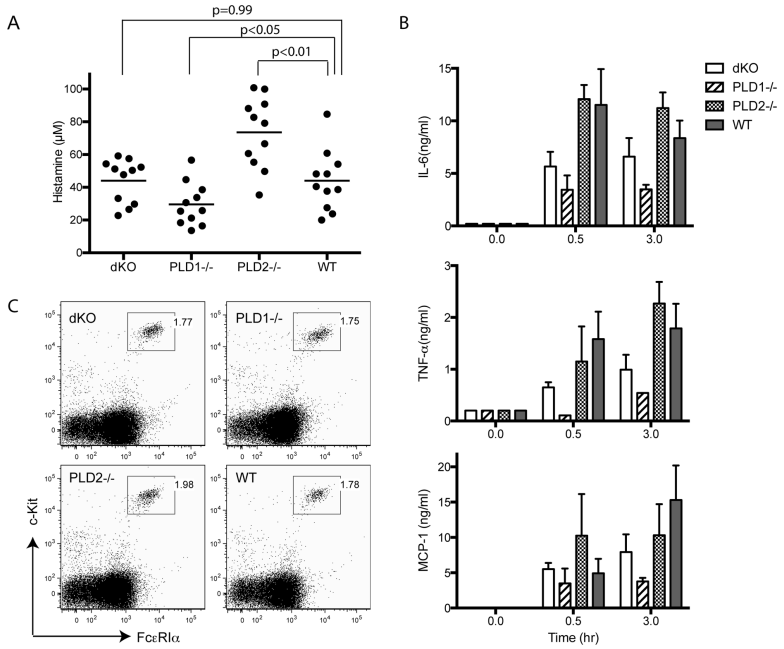

Figure 2.

PLD1 and PLD2 in mast cell function *in vivo*. (A). Passive systemic anaphylaxis. dKO, PLD1$^{-/-}$, PLD2$^{-/-}$, and WT mice were sensitized with 2μg of anti-DNP IgE for 20-24 hours. Anaphylaxis was induced by injection of 500 μg of DNP-HSA. Histamine concentration in the blood was determined by ELISA (n = 11 for each group of mice). The horizontal bars indicate mean values. Statistical analysis was done by two-tailed t test. (B). The levels of IL-6, TNF-α, and MCP-1. Mice were sensitized with 2 μg of anti-DNP IgE for 20-24 hours. Sera were collected 30 and 180 mins after injection of 500 μg of DNP-HSA. The concentrations of IL-6, TNF-α, and MCP-1 were determined by ELISA. (C). Expression of c-Kit and FcεRIα on peritoneal mast cells.

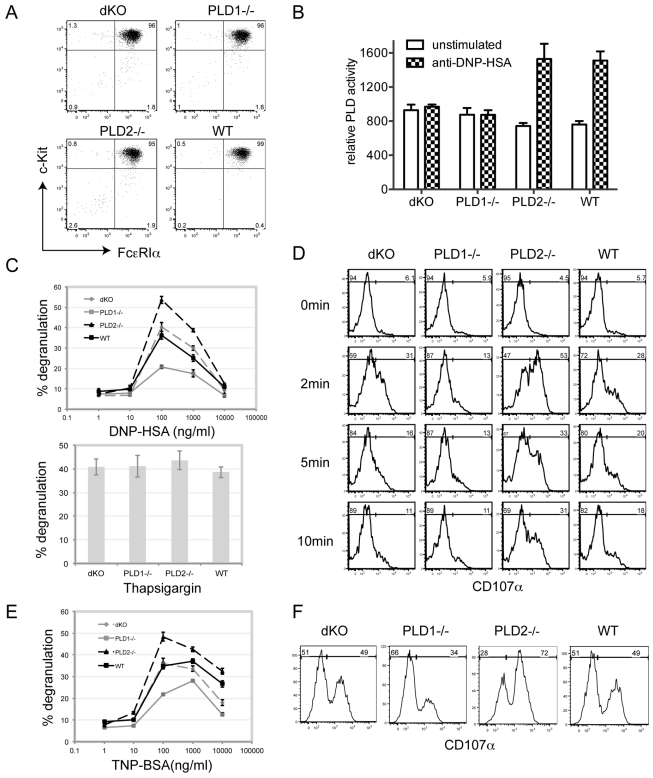

Figure 3.

PLD in mast cell function *in vitro*. Mast cells were derived from the bone marrow cells from dKO, PLD1$^{-/-}$, PLD2$^{-/-}$, and WT mice in the presence of IL-3 for three weeks before analysis. (A). Expression of c-Kit and FcεRIα on BMMCs. (B). The PLD deficiency on PLD activity in mast cells. (C). FcεRI-mediated degranulation. BMMCs were sensitized with 1 μg/ml of anti-DNP IgE and then stimulated with various concentrations of DNP-HSA for 10 min or with thapsigargin. Degranulation of BMMCs was determined by measuring the release of β-hexosaminidase in the culture supernatant. (D). FcεRI-induced up-regulation of CD107a surface expression. IgE-sensitized BMMCs were stimulated with 100ng/ml DNP-HSA for 0, 2, 5, and 10min before FACS analysis. (E). FcεRI-mediated degranulation using a poorly cytokinergic IgE. BMMCs were sensitized with 1 μg/ml of anti-TNP IgE (C48-2) and then stimulated with various concentrations of TNP-BSA for 10 min. Degranulation of BMMCs was determined by measuring the release of β-hexosaminidase into the culture supernatant. (F). FcεRI-induced up-regulation of CD107a surface expression. IgE (C48-2)-sensitized BMMCs were stimulated with 100ng/ml TNP-BSA for 5min before FACS analysis.

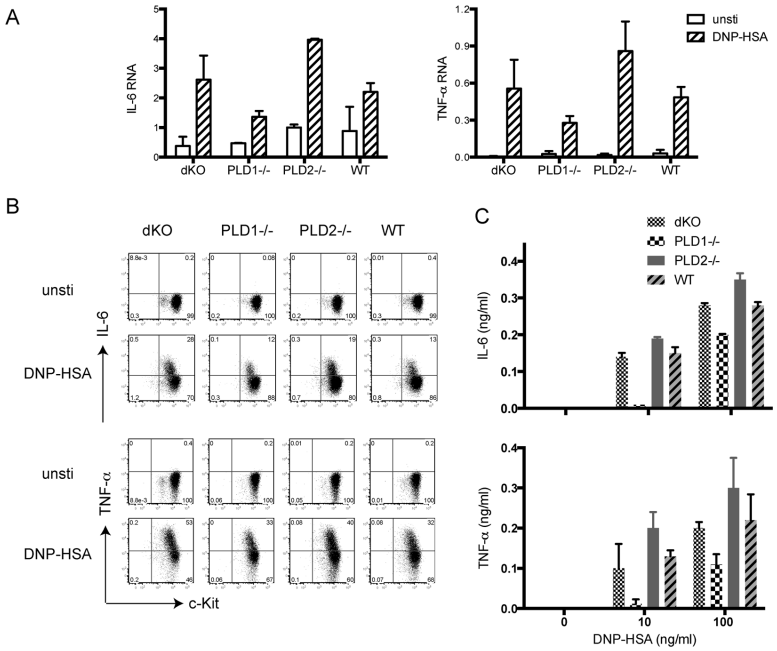

Figure 4. PLD in FcεRI-mediated cytokine production

(A). Real-time PCR analysis. IL-6 and TNF-α. Sensitized BMMCs were stimulated with 100 ng/ml DNP-HSA for 1 h or left untreated before RNA isolation. Relative levels of IL-6 and TNF-α RNAs were analyzed by real-time PCR. Data shown were normalized by GAPDH and are representative of three independent experiments. (B). Intracellular cytokine production. Sensitized BMMCs were stimulated with DNP-HSA (100 ng/ml) for 4 hours in the presence of monensin before intracellular staining for IL-6 and TNF-α. (C). IL-6 and TNF-α secretion. Sensitized BMMCs were stimulated with different concentration of DNP-HSA for 24 hours. IL-6 and TNF-α concentrations in the supernatant were measured by ELISA.

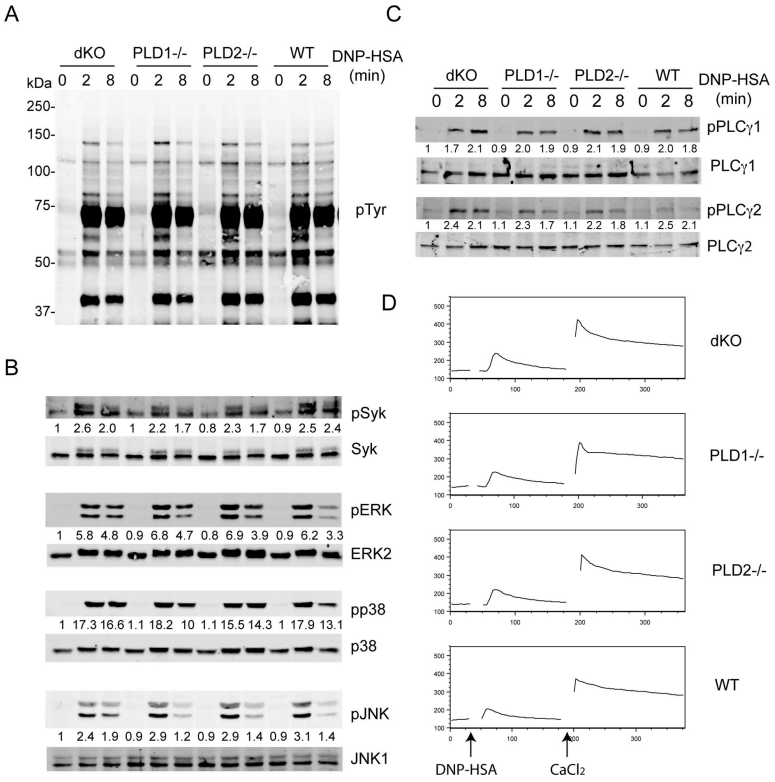

Figure 5.

The effect of PLD deficiency on FcεRI-mediated proximal signaling. (A). Tyrosine phosphorylation of proteins. After sensitization with anti-DNP IgE, dKO, PLD1$^{-/-}$, PLD2$^{-/-}$, and WT BMMCs were stimulated with DNP-HSA (100ng/ml) for the indicated time points. Whole cell lysates were analyzed by Western blotting with an anti-pTyr antibody. (B). MAPK activation. (C). PLC-γ activation. The numbers shown were relative intensities for the phosphorylated form of proteins normalized by non-phosphorylated form. (D). FcεRI-mediated calcium flux. BMMCs were sensitized with anti-DNP IgE and then loaded with Indo-1 in the presence of EGTA. DNP-HSA was used to induce intracellular Ca^{2+} mobilization followed by adding 20mM CaCl2 for extracellular Ca^{2+} flux. Data shown are representative of three experiments.

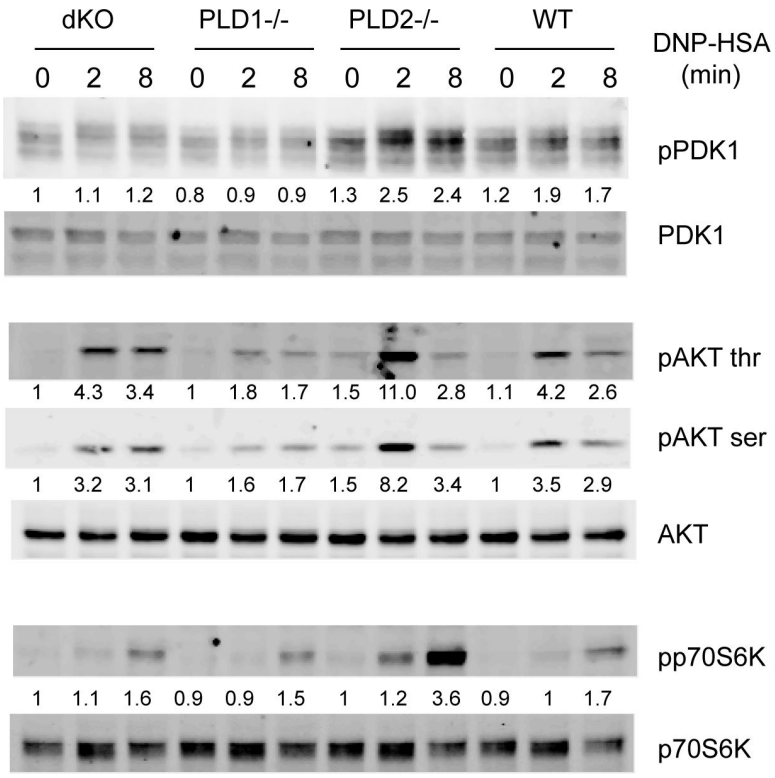

Figure 6.

The effect of PLD deficiency on the PI3K pathway. dKO, PLD1$^{-/-}$, PLD2$^{-/-}$, and WT BMMCs were sensitized with anti-DNP IgE and activated with DNP-HSA before lysis. Whole cell lysates were blotted with antibodies against the phosphorylated and non-phosphorylated forms of PDK1, p70S6K, and AKT. Data shown are representative of three experiments. The numbers shown were relative intensities for the phosphorylated form of proteins normalized by non-phosphorylated form.

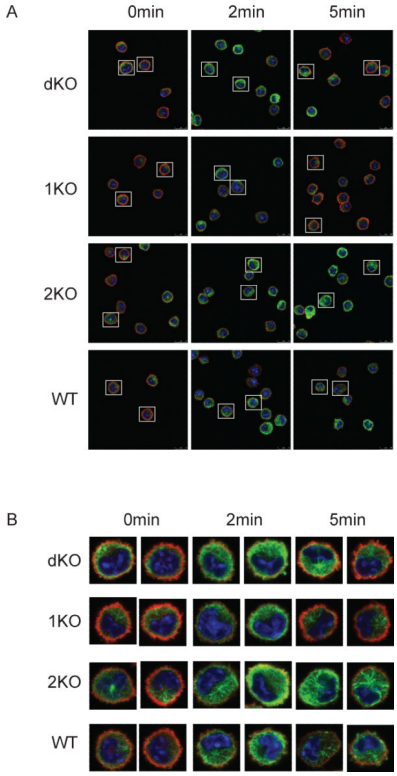

Figure 7.

PLD in FcεRI-mediated cytoskeletal rearrangement. (A). BMMCs were sensitized with anti-DNP IgE and then stimulated with DNP-HSA for 2 and 5 min. Cells were fixed and stained with anti–α-tubulin (green) and rhodamine-phalloidin (red). Representative images by the confocal microscopy are shown (A). (B). The enlarged images from two representative cells of each genotype.

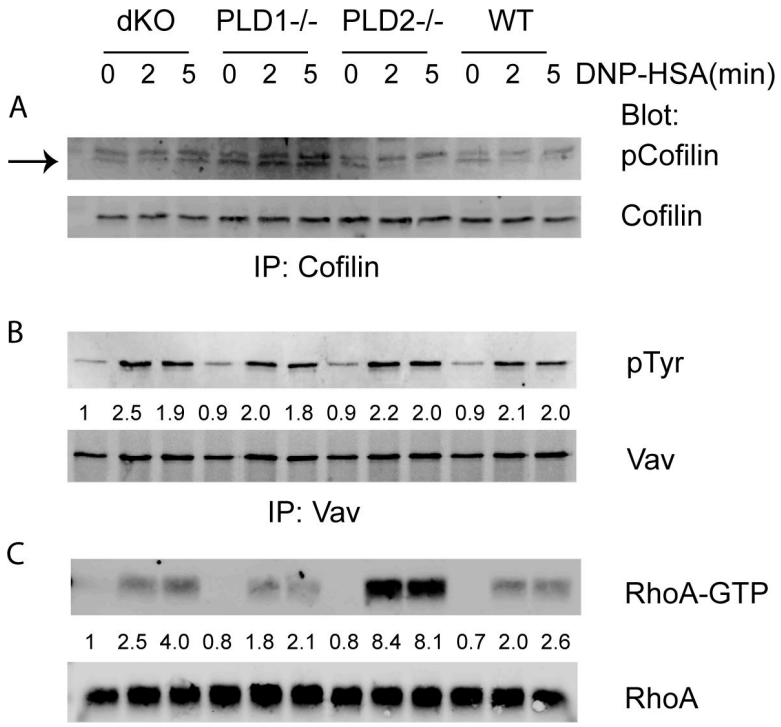

Figure 8.

PLD deficiency affects FcεRI-mediated RhoA activation in mast cells. BMMCs were stimulated with DNP-HSA for 2 and 5 min before lysis. (A). Dephosphorylation of cofilin after FcεRI engagement. Whole cell lysates were immunoprecipitated with anti-cofilin antibody, followed by blotting with anti-p-cofilin and anti-cofilin antibodies, respectively. (B). Normal Vav phosphorylation. (C). RhoA activation. The whole cell lysates were subjected to precipitation with GST-Rhotekin-RBD beads. RhoA in precipitates (top) and input lysates (bottom) was detected by Western blotting with anti-RhoA antibodies. One representative of three independent experiments is shown.